

## **Superconducting circuits and quantum computation**

### **Academic and Research Staff**

Professor Terry P. Orlando

### **Collaborators**

Prof. Leonid Levitov, Prof. Seth Lloyd, Prof. Johann E. Mooij<sup>1</sup>, Dr. Juan J. Mazo<sup>2</sup>, Dr. Fernando F. Faló<sup>2</sup>, Dr. Karl Berggren<sup>3</sup>, Prof. M. Tinkham<sup>4</sup>, Nina Markovic<sup>4</sup>, Sergio Valenzuela<sup>4</sup>, Prof. Marc Feldman<sup>5</sup>, Prof. Mark Bocko<sup>5</sup>, Jonathon Habif<sup>5</sup>, Dr. Enrique Trías

### **Visiting Scientists and Research Affiliates**

Dr. Juan Mazo<sup>2</sup>, Prof. Johann E. Mooij<sup>1</sup>, Dr. Kenneth J. Segall, Dr. Enrique Trías

### **Graduate Students**

Donald S. Crankshaw, Daniel Nakada, Lin Tian, Janice Lee, Bhuwan Singh, David Berns, William Kaminsky, Bryan Cord

### **Undergraduate Students**

Andrew Cough

### **Support Staff**

Scott Burris

### **Introduction**

Superconducting circuits are being used as components for quantum computing and as model systems for non-linear dynamics. Quantum computers are devices that store information on quantum variables and process that information by making those variables interact in a way that preserves quantum coherence. Typically, these variables consist of two quantum states, and the quantum device is called a quantum bit or qubit. Superconducting quantum circuits have been proposed as qubits, in which circulating currents of opposite polarity characterize the two quantum states. The goal of the present research is to use superconducting quantum circuits to perform the measurement process, to model the sources of decoherence, and to develop scalable algorithms. A particularly promising feature of using superconducting technology is the potential of developing high-speed, on-chip control circuitry with classical, high-speed superconducting electronics. The picosecond time scales of this electronics means that the superconducting qubits can be controlled rapidly on the time scale and the qubits remain phase-coherent.

Superconducting circuits are also model systems for collections of coupled classical non-linear oscillators. Recently we have demonstrated a ratchet potential using arrays of Josephson junctions as well as the existence of a novel non-linear mode, known as a discrete breather. In addition to their classical behavior, as the circuits are made smaller and with less damping, these non-linear circuits will go from the classical to the quantum regime. In this way, we can study the classical-to-quantum transition of non-linear systems.

---

<sup>1</sup> Delft University of Technology, The Netherlands

<sup>2</sup> University of Saragoza, Spain

<sup>3</sup> M.I.T. Lincoln Lab

<sup>4</sup> Harvard University

<sup>5</sup> University of Rochester

## 1. Superconducting Persistent Current Qubits in Niobium

### Sponsors

AFOSR grant F49620-1-1-0457 funded under the Department of Defense, Defense University Research Initiative on Nanotechnology (DURINT) and by ARDA

### Project Staff

Ken Segall, Daniel Nakada, Donald Crankshaw, Bhuwan Singh, Janice Lee, Bryan Cord, Karl Berggren (Lincoln Laboratory), Nina Markovic and Sergio Valenzuela (Harvard); Professors Terry Orlando, Leonid Levitov, Seth Lloyd and Professor Michael Tinkham (Harvard)

Quantum Computation is an exciting idea whose study combines the exploration of new physical principles with the development of a new technology. In these early stages of research one would like to be able to accomplish the manipulation, control and measurement of a single two-state quantum system while maintaining quantum coherence. This will require a coherent two-state system (a qubit) along with a method of control and measurement. Superconducting quantum computing has the promise of an approach that could accomplish this in a manner that can be scaled to large numbers of qubits. We are studying the properties of a two-state system made from a niobium (Nb) superconducting loop, which can be incorporated on-chip with other superconducting circuits to perform the control and measurement. The devices we study are fabricated at Lincoln Laboratory, which uses a Nb-trilayer process for the superconducting elements and photolithography to define the circuit features. Our system is thus inherently scalable but has the challenge of being able to demonstrate appreciable quantum coherence.

The particular device that we have studied so far is made from a loop of Nb interrupted by 3 Josephson junctions (Fig. 1a). The application of an external magnetic field to the loop induces a circulating current whose magnetic field either adds to (say circulating current in the clockwise direction) or opposes (counterclockwise) the applied magnetic field. When the applied field is near to one-half of a flux quantum, both the clockwise and counterclockwise current states are classically stable. The system behaves as a two-state system. The potential energy versus circulating current is a so-called double-well potential (see Fig.2), with the two minima representing the two states of equal and opposite circulating current.

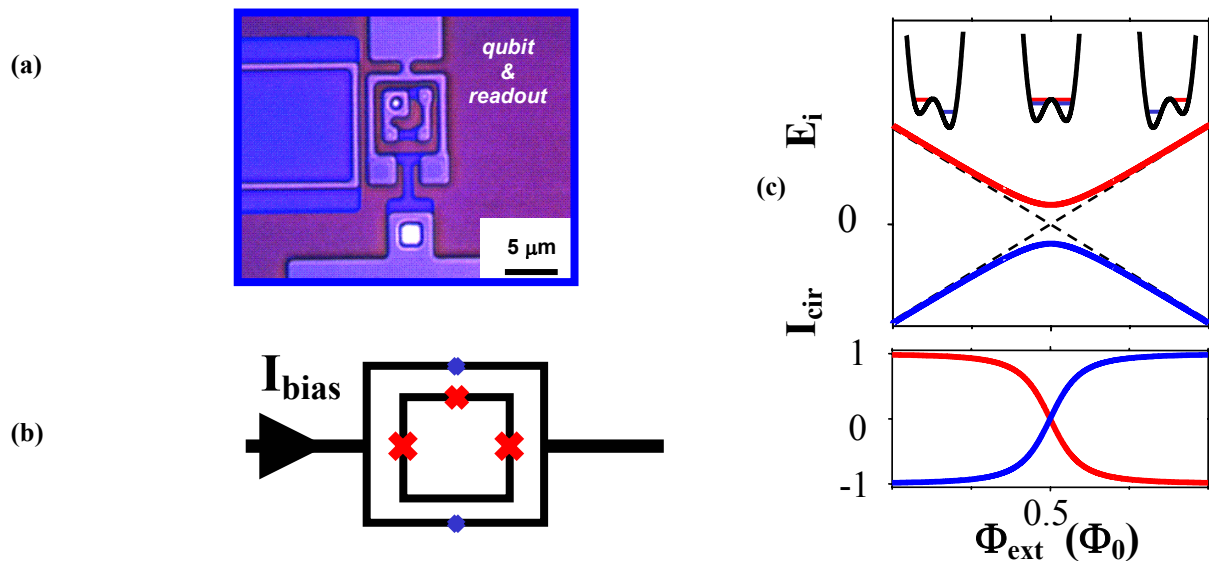


**Figure 1:** (a) SEM image of the persistent current qubit (inner loop) surrounded by the measuring dc SQUID. (b) a schematic of the qubit and measuring SQUID, the x's mark the Josephson junctions. (c) The energy levels for the ground state (dark line) and the first excited state of the qubit versus applied

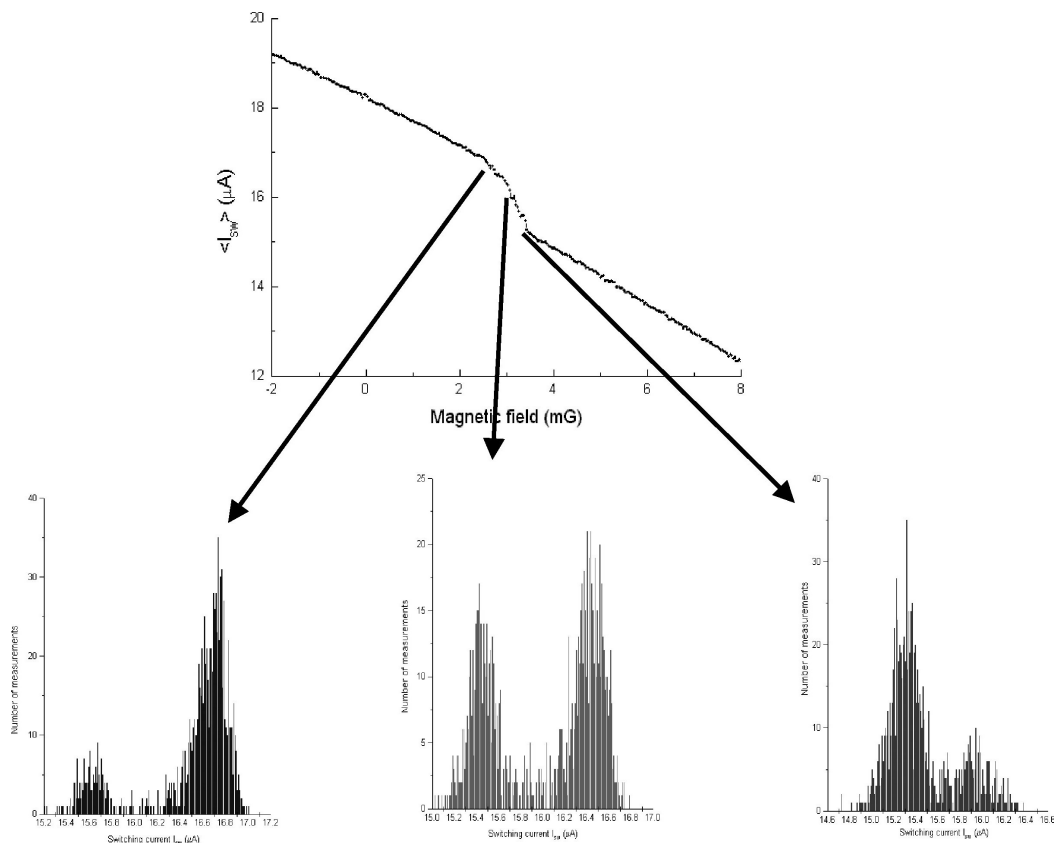
flux. The double well potentials are shown schematically above. The lower graph shows the circulating current in the qubit for both states as a function of applied flux. The units of flux are given in terms of the flux quantum.

Figure 1a shows a SEM image of the persistent current qubit (inner loop) and the measuring dc SQUID (outer) loop. The Josephson junctions appear as small “breaks” in the image. A schematic of the qubit and the measuring circuit is shown in Figure 1b, where the Josephson junctions are denoted by x's. The sample is fabricated at MIT's Lincoln Laboratory in niobium by photolithographic techniques on a trilayer of niobium-aluminum oxide-niobium wafer

The energy levels of the ground state (dark line) and the first excited state (light line) are shown in Figure 1c near the applied magnetic field of  $0.5 \Phi_0$  in the qubit loop. Classically the Josephson energy of the two states would be degenerate at this bias magnetic field and increase and decrease linearly from this bias field, as shown by the dotted line. Since the slope of the  $E$  versus magnetic field is the circulating current, we see that these two classical states have opposite circulating currents. However, quantum mechanically, the charging energy couples these two states and results in a energy level repulsion at  $\Phi_{\text{ext}} = 0.5 \Phi_0$ , so that there the system is in a linear superposition of the currents flowing in opposite directions. As the applied field is changed from below  $\Phi_{\text{ext}} = 0.5 \Phi_0$  to above, we see that the circulating current goes from negative, to zero at  $\Phi_{\text{ext}} = 0.5 \Phi_0$ , to positive as shown in the lower graph of Figure 1c. This flux can be measured by the sensitive flux meter provided by the dc SQUID.

A SQUID magnetometer inductively coupled to the qubit can be used to measure the magnetic field caused by the circulating current and thus determine the state of the qubit. The SQUID has a switching current which depends very sensitively on magnetic field. When the magnetic field from the qubit adds to the external field we observe a smaller switching current; when it subtracts from the external field we observe a smaller larger current. We measure the switching current by ramping up the bias current of the SQUID and recording the current at which it switches. Typically a few hundred such measurements are taken. We have performed these measurements versus magnetic field, temperature and SQUID ramping rate.

In the upper plot of Fig. 2 we show the average switching current versus magnetic field for our qubit-SQUID system. The SQUID switching current depends linearly on the applied magnetic field. A step-like transition occurs when the circulating current in the qubit changes sign, hence changing whether its magnetic field adds to or subtracts from the applied field. In Fig. 1 the qubit field adds to the SQUID switching current at lower fields ( $< 3\text{mG}$ ) but subtracts from it at higher fields ( $> 3\text{mG}$ ). Each point in the upper curve is an average of 1000 single switching current measurements. If we look at a histogram of the 1000 switching currents in the neighborhood of the transition, we discover that it represents a joint probability distribution. Two distinct switching currents representing the two states of the qubit can be clearly resolved. Changing the magnetic field alters the probability of being measured in one state or the other.



**Fig. 2:** Measurements of the switching current of the SQUID versus magnetic field.

In Fig. 3 we show the potential energy for the system as we sweep through the transition. (We used a different assignment for “zero” field in Fig. 3 than Fig. 2, which is why the step occurs at a different magnetic field value). In the first part of the transition the system has a higher probability of being measured in the left well, which corresponds to the circulating current state which adds to switching current of the SQUID. At the midpoint of the transition the system is measured in both wells with equal probability. At higher fields the system has a larger probability of being measured in the right well. The mechanism for the system to move between the wells at these temperatures ( $>300$  mK) is thermal activation. We have measured the system at lower temperatures, and there the mechanism is unclear. The focus of our future efforts is to determine if the mechanism changes to quantum mechanical tunneling at lower temperatures and how coherent the tunneling can be. If we are successful that will be the first indication that superconducting quantum computers in Nb are possible.

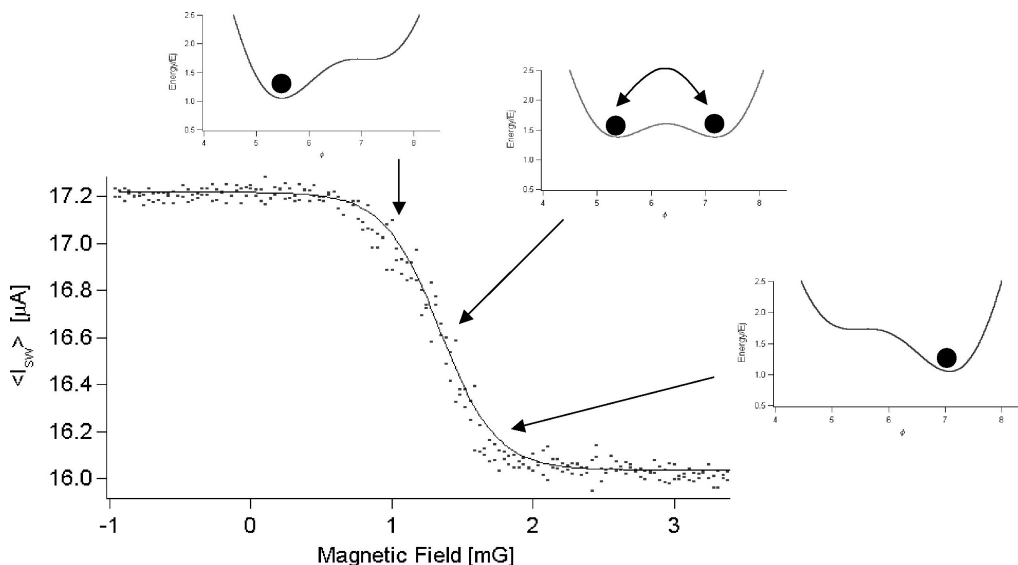


Fig. 3: Switching current versus magnetic field with the background field of the SQUID subtracted off.

## 2. Thermal Activation Characterization of Qubits

### Sponsors:

AFOSR grant F49620-1-1-0457 funded under the Department of Defense, Defense University Research Initiative on Nanotechnology (DURINT) and by ARDA

### Project Staff:

Ken Segall, Daniel Nakada, Donald Crankshaw, Bhuwan Singh, Janice Lee, Karl Berggren, Nina Markovic and Sergio Valenzuela; Professors Terry Orlando, Leonid Levitov, Seth Lloyd and Michael Tinkham

In our work we have demonstrated two distinct measurable states of the qubit, have observed thermal activation between the two states, and have seen an effect where the measurement device acts on the qubit, an effect that we refer to as time-ordering of the measurements.

The PC qubit is surrounded by a two-junction DC-SQUID magnetometer, which reads out the state of the PC qubit. The SQUID is highly underdamped, so the method of readout is to measure its switching current, which is sensitive to the total flux in its loop. A bias current  $I_b$  was ramped from zero to above the critical current of the SQUID, and the value of current at which the junction switched to the gap voltage was recorded for each measurement (see Fig. 1b-c). The repeat frequency of the bias current ramp was varied between 10 and 150 Hz. Typically several hundred measurements were recorded, since the switching is a stochastic process. The experiments were performed in a pumped  $^3\text{He}$  refrigerator, at temperatures of 330 mK to 1.2 K. A magnetic field was applied perpendicular to the sample in order to flux bias the qubit near to one half a flux quantum in its loop.

The PC qubit biased near half a flux quantum can be approximated as a two-state system, where the states have equal and opposite circulating current. These two states will be labeled **0** and **1**. The circulating current in the qubit induces a magnetization into the SQUID loop equal to  $MI_{circ}$ , where  $M$  is the mutual inductance between the qubit and the SQUID and  $I_{circ}$  is the circulating current in the qubit. The two different circulating current states of the qubit cause two different switching currents in the SQUID. Without loss of generality we can call **0** the state corresponding to the smaller switching current and **1** the state corresponding to the larger switching current. A central aspect of the measurement is that it takes a finite time to be completed. The current  $I_b(t)$  passes the smaller switching current at time  $t_0$  and the larger

switching current at a later time  $t_1$  (Fig. 1c); measurement of state **0** occurs before measurement of state **1**. This we refer to as time-ordering of the measurements. We call  $\tau = (t_1 - t_0)$  the measurement time. Thermal activation of the system *during* time  $\tau$  causes a distinct signature in the data and allows us to measure the thermal activation rate.

The average switching current as a function of magnetic field is shown in Fig. 2. The transfer function of the SQUID has been subtracted off, leaving only the magnetization signal due to the qubit. At low magnetic fields (to the left in Fig. 2), the system is found only in the **0** state, corresponding to the lower switching current. As the magnetic field is increased, the system probability is gradually modulated until it is found completely in the **1** state, corresponding to the larger switching current. Focusing on the point in flux where the two states are equally likely, one can see that it is formed from a bimodal switching distribution, with the two peaks corresponding to the two different qubit states.

In Fig. 2 we also show the best fit for each curve from our model. The same fitting parameters are used in both cases, with only the temperature allowed to vary. The 0.62 K curve has moved in flux relative to the 0.33 K curve, as expected. The theory predicts both the curve's shape and its relative position in flux. We use this agreement to fit the parameters of our system. There are three fitting parameters for the model to fit the data:  $E_J$ ,  $\alpha$  and  $Q$ .  $E_J$  is the Josephson energy for each of the two larger junctions in the three-junction qubit, which, for a given current density, is proportional to their physical size. The parameter  $\alpha$  is the ratio of the smaller junction to the two larger ones, as previously mentioned. The damping factor  $Q$  is associated with thermal activation from the **1** to the **0** state in equation (3). The value of  $E_J$  which best fits the data is 4000  $\mu\text{eV}$ . This corresponds to a size of about 0.52  $\mu\text{m} \times 0.52 \mu\text{m}$  for each of the two larger junctions. The values of  $\alpha$  was found to be 0.58, corresponding to a smaller junction size of 0.39  $\mu\text{m}$ . These values are quite reasonable given the fabrication of our junctions. The larger junctions are lithographically 1  $\mu\text{m}$  in length while the smaller junctions are lithographically 0.9  $\mu\text{m}$ ; however, the fabrication process results in a sizing offset of between 0.4 and 0.55  $\mu\text{m}$ , measured on similar structures.

The value of  $Q$  is found to be  $1.2 \times 10^6$ , with an uncertainty of about a factor of 3, given the sources of error in the measurement and the fitting. This value corresponds to a relaxation time of roughly  $Q/\omega_0 \sim 1 \mu\text{s}$ . Similar relaxation times have been measured in aluminum superconducting qubits, and indicate possible long coherence times in the quantum regime. The value of  $10^6$  is consistent with a subgap resistance of 10  $\text{M}\Omega$  measured in similar junctions. The inferred relaxation time is also consistent with the calculated circuit impedance. This inferred value of  $Q$  is important for the long-term prospects of our qubits, as it indicates that it is possible to obtain very low dissipation in our structures.

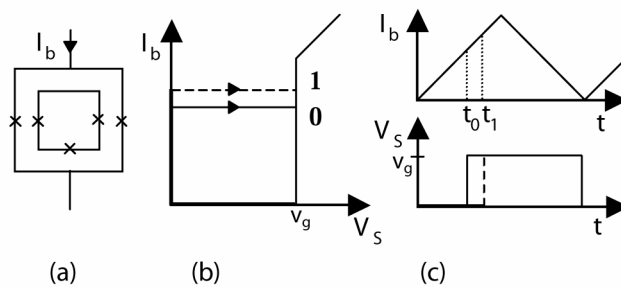


**Fig. 1:** (a) Schematic of the PC qubit surrounded by a DC SQUID. The X's represent junctions. (b) Schematic curve of the bias current ( $I_b$ ) vs. the SQUID voltage ( $V_s$ ) for the SQUID. At the switching point the SQUID voltage switches to the gap voltage  $v_g$ . The **0** and **1** qubit states cause two different switching currents. (c) Timing of the current and voltage in the SQUID as the measurement proceeds. If the qubit is in state **0**,  $V_s$  switches to  $v_g$  at time  $t_0$ ; if the qubit is in state **1**,  $V_s$  switches at time  $t_1$ . The time difference  $t_1 - t_0$  forms a timescale for the measurement.

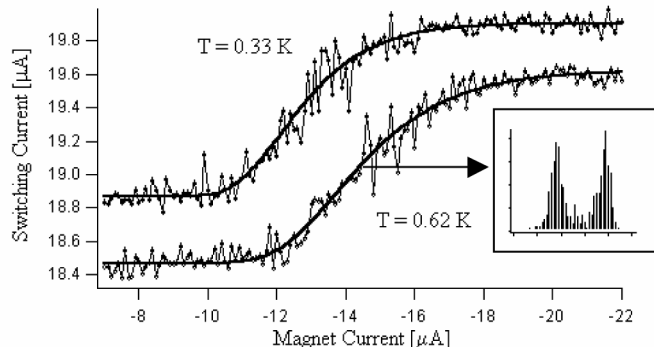


**Fig. 2:** Switching current versus magnetic field for device A for bath temperatures of  $T = 0.33$  K and  $T = 0.62$  K. The 0.33 K curve is intentionally displaced by  $0.3 \mu\text{A}$  in the vertical direction for clarity. The model (equation (7)), with fitted temperature values of 0.38 K and 0.66 K, fits the data well, describing accurately the dependence of both the location of the midpoint of the transition and the shape of the transition on the device temperature. Inset shows a histogram for a flux bias where the system is found with equal probability in either state. The distribution is bimodal, showing the two states clearly.

### 3. Improved Critical-Current-Density Uniformity of Nb Superconducting Fabrication Process by Using Anodization

#### Personnel

Daniel Nakada<sup>1</sup>, Karl K. Berggren<sup>2</sup>, Earle Macedo<sup>2</sup> (T.P. Orlando<sup>1</sup>)

<sup>1</sup>MIT, Department of Electrical Engineering and Computer Science

<sup>2</sup>MIT Lincoln Laboratory, Lexington, MA 02420

#### Sponsorship

DOD, ARDA, ARO, AFOSR

We developed an anodization technique for a Nb/Al/AIO<sub>x</sub>/Nb superconductive-electronics-fabrication process that results in an improvement in critical-current-density  $J_c$  uniformity across a 150-mm-diameter wafer. The superconducting Josephson junctions studied were fabricated in a class-10 cleanroom facility at MIT Lincoln Laboratory. The Nb superconducting process uses optical projection lithography, chemical mechanical planarization of two oxide layers, a self-aligned via process and dry reactive ion etching (RIE) of the Nb and oxide layers. The most critical step in the fabrication process however is the definition of the tunnel junction. The junction consists of two Nb layers, the base electrode (B.E.) and counter-electrode (C.E.) separated by a thin AIO<sub>x</sub> barrier. Fig. 1a shows a cross-section of the Josephson junction region after RIE is performed on the counter-electrode. After RIE, the junction region could be vulnerable to chemical, plasma and/or other damage from subsequent processing steps, we therefore anodized the wafer to form a 50-nm-thick protective metal-oxide layer around the junction perimeter. Anodization is an electrolytic process in which the surface of a metal is converted to its oxide form, this metal oxide layer serves as a protective barrier to further ionic or electron flow. Fig.1b shows that after anodization the junction region is “sealed” from the outside environment by a thick NbO<sub>x</sub> layer. Anodization is useful in minimizing damage to the junction region. We also used transmission electron microscopy (TEM) images to inspect the anodic film (Fig 2a, b).

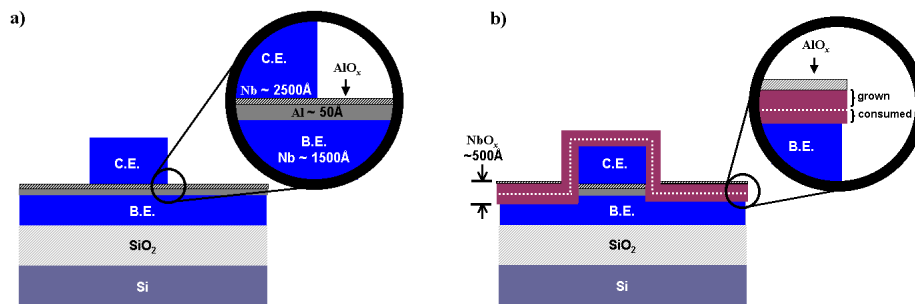


**Fig. 1a)** Nb Josephson junction after counter-electrode (C.E.) etch but immediately prior to anodization. Inset shows thin AlO<sub>x</sub> barrier vulnerable to outside environment. b) Junction region after anodization. The surface of the counter and base-electrode (B.E.) is converted to a metal-oxide layer approximately 500 Å thick. The dotted line shows the original surface. Inset shows amount of anodic oxide grown and consumed. The anodic oxide causes the surface to swell up and out slightly during growth.

This work was sponsored by the Department of Defense under the Department of the Air Force contract number F19628-00-C-0002. Opinions, interpretations, conclusions and recommendations are those of the author and are not necessarily endorsed by the Department of Defense.

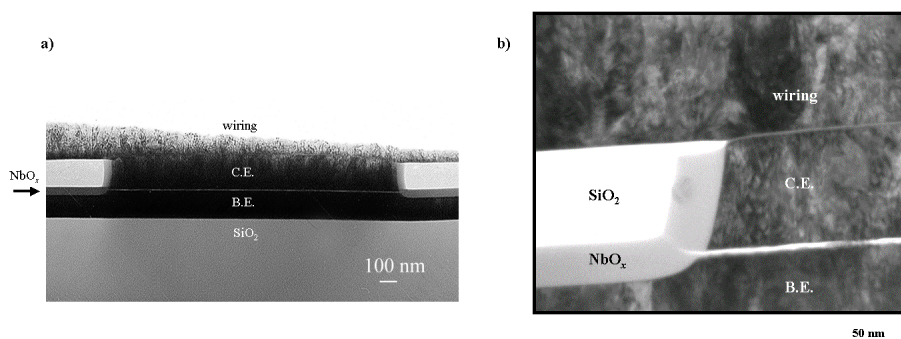


**Fig.2a)** TEM image of an anodized junction showing clearly the sealing of the junction edge by NbO<sub>x</sub>. Note the clean interface between the counter-electrode and wiring layer where the NbO<sub>x</sub> has been removed by CMP. b) TEM image shows AlO<sub>x</sub> barrier within the NbO<sub>x</sub> layer.

Critical current  $I_c$  measurements of Josephson junctions were performed at room temperature using specially designed test structures. We used an automatic probing station to determine the  $I_c$  values of junctions distributed across an entire wafer. We then compared the  $J_c$  uniformity of pairs of wafers, fabricated together, differing only in the presence or absence of the anodization step. The cross-wafer standard deviation of  $J_c$  was typically ~ 5% for anodized wafers but > 15% for unanodized wafers (Fig. 3). Overall, unanodized wafers had a factor of ~ 3 higher standard deviation compared to anodized wafers. A low variation in  $J_c$  results in a higher yield of device chips per wafer with the desired current density. As a result of the improved cross-wafer distribution, the cross-chip uniformity is greatly improved as well; typically < 1% for anodized chips. Control of  $J_c$  is important for all applications of superconductive electronics including quantum computation and rapid single-flux quantum (RSFQ) circuitry.

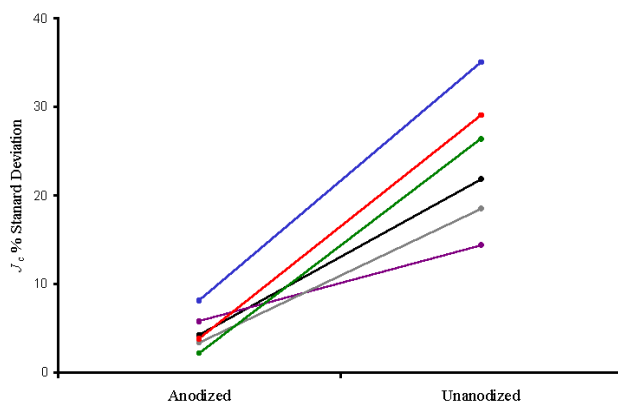


**Fig. 3:** Comparison of cross-wafer critical-current-density standard deviation of anodized / unanodized wafer pairs. The wafers shown have  $J_c$  values ranging between  $10^2 \text{ A/cm}^2$  and  $10^3 \text{ A/cm}^2$ . Lines connect data points on wafers whose trilayers were deposited together.

#### 4. On-chip Oscillator coupled to the Qubit: Design and Experiments to Reduce Decoherence

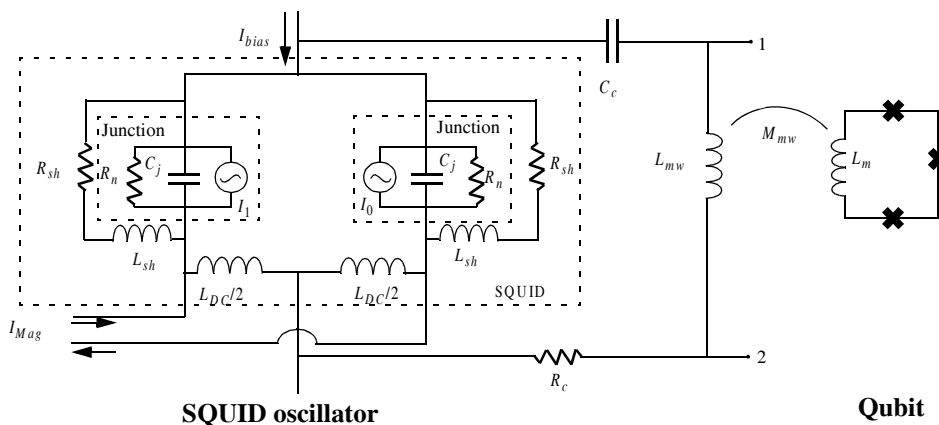


**Figure 1:** Circuit diagram of the SQUID oscillator coupled to the qubit. The SQUID contains two identical junctions, here represented as independent current sources and the RCSJ model, shunted by a resistor and inductor ( $R_{sh}$  and  $L_{sh}$ ). A large superconducting loop ( $L_c$ ) provides the coupling to the qubit. The capacitor,  $C_c$ , prevents the dc current from flowing through this line, and the resistance,  $R_c$ , damps the resonance.  $Z_t$ , the impedance seen by the qubit, is the impedance across the inductor,  $Z_{12}$ .

The oscillator in Figure 1 is a simple overdamped dc SQUID which acts as the on-chip oscillator which drives the qubit. This gives two parameters with which to control the frequency and amplitude of the oscillator: the bias current and the magnetic flux through the SQUID. In this design, the SQUID is placed on a ground plane to minimize any field bias from an external source, and direct injection supplies the flux by producing excess current along a portion of the SQUID loop. When a Josephson junction is voltage biased, its current oscillates at a frequency of  $V_{bias}/\Phi$  with an amplitude of  $I_c$ . For a stable voltage bias, this looks like an independent ac current source. In this circuit, the junction is current biased, and its oscillating output produces fluctuations in the voltage across the junction. Thus the dc voltage, approximately equal to  $I_{bias}R_{sh}$ , gives the fundamental frequency, while harmonics distort the signal. If the

shunt is small, such that  $V_{bias} \gg I_c |R_{sh} + j\omega L_{sh}|$ , the voltage oscillations are small relative to the dc voltage and the higher harmonics become less of a problem. This allows us to model the junctions as independent sources ( $I_0$  and  $I_1$ ) in parallel with the RCSJ model. A dc SQUID with a small self inductance behaves much like a single junction whose  $I_c$  can be controlled by the flux through its loop. The circuit model is shown in Figure 1. This is similar in concept to our previous work with Josephson array oscillators. The impedance seen by the qubit is given by placing the other elements of the circuit in parallel with the inductance. The maximum amplitude of the oscillating magnetic flux is at the resonance of the RLC circuit consisting of  $R_c$ ,  $C_c$ , and  $L_c$ . In this case, the LC resonance occurs at 8.6 GHz. Directly on resonance, the SQUID produces high amplitude oscillations with a short dephasing time. Moving it off resonance lowers the amplitude but lengthens the dephasing time, as shown in Figure 2.

Table 1. SQUID oscillator parameters

$I_c$	$R_n$	$C_j$	$R_{sh}$	$L_{sh}$	$R_c$	$C_c$	$L_c$	$M_c$
260 $\mu$ A	7.3 $\Omega$	2100 fF	0.19 $\Omega$	0.38 pH	0.73 $\Omega$	4600 fF	75 pH	0.6 pH

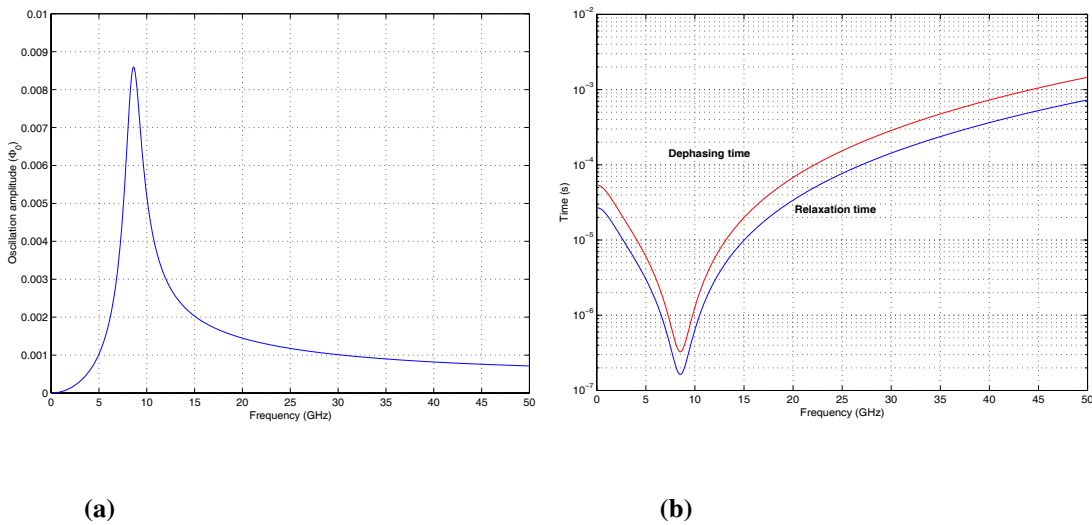
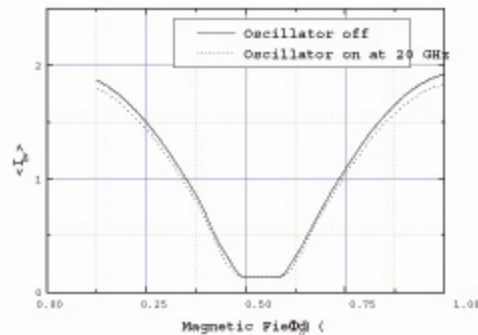


Figure 2: Graphs showing the amplitude produced by the oscillator (a) and the decoherence times caused by the oscillator (b) as a function of frequency.



**Figure 3:** This graph shows the switching current of the DC SQUID while the oscillator is off and while it is on. The current is clearly suppressed by turning the oscillator on.

This oscillator has been fabricated and testing has begun. Although it is too early to comment on its effect on the qubit, it is clear that the oscillator is producing sufficient signal to suppress the current of the dc SQUID magnetometer used to measure the qubit's state, as shown in Figure 3.

## 5. Projective Measurement Scheme for Solid-State Qubits

### Sponsors

Department of Defense University Research Initiative on Nanotechnology (DURINT) Grant F49620-01-1-0457

### Project Staff

Lin Tian, Professor Seth Lloyd, Professor Terry P. Orlando

Effective measurement for quantum bits is a crucial step in quantum computing. An ideal measurement of the qubit is a projective measurement that correlates each state of the quantum bit with a macroscopically resolvable state. In practice, it is often hard to design an experiment that can both projectively measure a solid-state qubit effectively and meanwhile does **not** couple environmental noise to the qubit. Often in solid-state systems, the detector is fabricated onto the same chip as the qubit and couples with qubit all the time. On the one hand, noise should not be introduced to the qubit via the coupling with the detector. This requires that the detector is a quantum system well-isolated from the environment. On the other hand, to correlate the qubit states to macroscopically resolvable states of the detector, the detector should behave as classical system that has strong interaction with the environment, and at the same time interacts with the qubit strongly. These two aspects contradict each other, hence measurements on solid-state quantum bits are often limited by the trade-off between these two aspects. In the first experiment on the superconducting persistent-current qubit (pc-qubit), the detector is an under-damped dc SQUID that is well-isolated from the environment and behaves quantum mechanically. The detected quantity of the qubit- the self-induced flux, is small compared with the width of the detector's wave packet. As a result, the detector has very bad resolution in the qubit states. This is one of the major problems in the study of the flux-based persistent-current qubits.

Various attempts have been made to solve the measurement problem. We present a new scheme in Figure 1 that effectively measures the pc-qubit by an on-chip detector in a "single-shot" measurement and does not induce extra noise to the qubit until the measurement is switched on. The idea is to make a switchable measurement (but a fixed detector) that only induces decoherence during the measurement. During regular qubit operation, although the qubit and the detector are coupled, the detector stays in its ground state and only induces an overall random phase to the qubit. The measurement process is then

switched on by resonant microwave pulses. First we maximally entangle the qubit coherently to a supplementary quantum system. Then we measure the supplementary system to obtain the qubit's information.

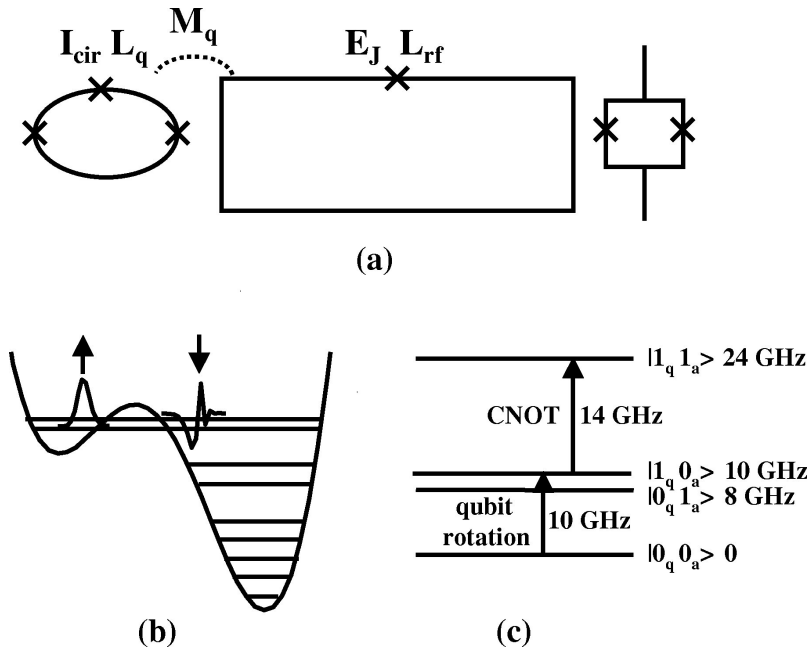


**Fig. 1:** (a). The circuit for the measurement scheme, from left to right: the qubit, the rf SQUID and the dc SQUID magnetometer. The pc-qubit couples with the rf SQUID via the mutual inductance  $M_q$ . (b). Energy levels of rf SQUID with its potential energy when biased at  $f_{rf} = 0.4365$  flux quantum. The effective two-level system (ETLS) are labeled with arrows and their wave functions are shown. (c). The states of the interacting qubit and the rf SQUID. The energies are in units of GHz.

## 6. Fast On-chip Control Circuitry

### Sponsors

ARO Grant DAAG55-98-1-0369 and Department of Defense University Research Initiative on Nanotechnology (DURINT) Grant F49620-01-1-0457

### Project Staff

Donald S. Crankshaw, John Habif, Daniel Nakada, Professor Marc Feldman, Professor Mark Bocko, Dr. Karl Berggren

RSFQ (Rapid Single Flux Quantum) electronics can provide digital circuitry which operates at speeds ranging from 1 - 100 GHz. It uses a voltage pulse to indicate a 1 and the lack of a voltage pulse within a clock cycle indicates a 0. If these electronics can be integrated onto the same chip as the qubit, complicated control with precise timing can be applied to the qubit by on-chip elements. The following design is currently in fabrication.

An RSFQ clock can be used as the oscillator to rotate the PC qubit. This oscillator has more frequency components and less tunability than a dc SQUID, but it is easier to use in conjunction with other RSFQ components. In the following design, these components can deliver a variable frequency signal. An RSFQ clock is simply a Josephson Transmission Line ring. The transmission line propagates a pulse in its loop, which can be tapped off and used as a clock signal. Two counters and a Non-Destructive Read

Out (NDRO) memory cell make up the digital pulse width modulator. The signal from the clock goes to both counters and to the Read input of the NDRO. The NDRO outputs a 1 for each clock input if a 1 is stored in it, but no output for each pulse if a 0 is stored in it. The output of the counters go to the Set (which sets the NDRO to 1) and the Reset (which resets the NDRO to 0) inputs of the NDRO. The counters are equal in length (13 bits), so that after  $2^{13}$  pulses, each one sends its output to the NDRO. By initially offsetting the counters by preloading them with the Offset inputs, one can set them out-of-phase with one another, thus controlling the duty cycle of the NDRO output. Since the NDRO signal has lots of harmonics, an RLC resonance filters the signal before delivering it to the qubit. The resonance filter converts the highly non-linear clock signal to a nearly sinusoidal signal.

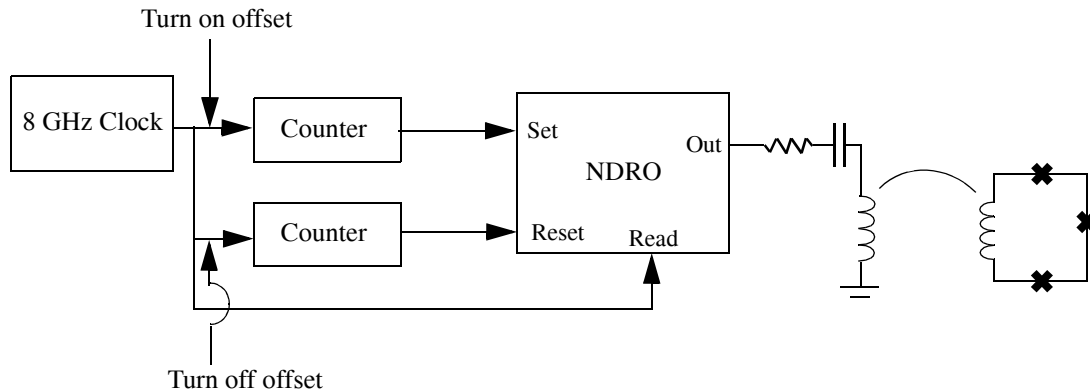


**Figure 1:** An RSFQ Variable Duty Cycle Oscillator.

The design has been fabricated, although testing is not yet complete. The most likely difficulty is easily identified given the results presented in Sections 2 and 3. Both the RSFQ circuit and the qubit have been fabricated at a current density of  $500 \text{ A/cm}^2$ , where the qubit does not display the desired quantum properties. A new design is needed for  $100 \text{ A/cm}^2$ , which is where the qubit parameters are more ameliatory. This is shown in Figure 5. This design is simpler, since  $100 \text{ A/cm}^2$  requires larger junction and inductor sizes, which lessens circuit density, and it operates more slowly. In this case, the timing is done off-chip, which is beneficial for synchronizing the measurement with the driving. The oscillator is once again a Josephson transmission line ring, this time operating at 3 GHz, and a signal is tapped off to drive the qubit. This time there is no intervening circuitry, so the qubit sees an oscillating signal as long as the clock is on. The clock is interrupted by a NOT gate. Every time the clock ring sends its signal to the NOT gate, it will send a signal back into the ring unless it has received an external signal, in which case it will not output a pulse and the clock will turn off. The signal which stops the clock comes from off the chip, using a single T-flip-flop as a divider. The first signal which comes from off-chip will be sent by the T-flip-flop to start the clock, while the second signal will be sent to stop it.

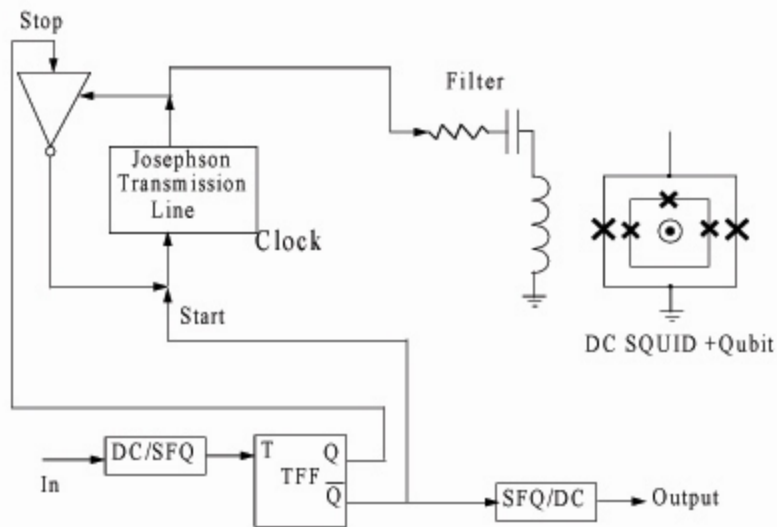


**Figure 2:** An RSFQ oscillator which may be turned on and off by an external signal.

## 7. Design of Coupled Qubit

### Sponsors

ARO Grant DAAD-19-01-1-0624 and Hertz Fellowship

### Project Staff

Bhuvan Singh, John Habib, William Kaminsky, Professor Terry Orlando, Professor Seth Lloyd

The main requirement for the coupled qubits is that the coupled qubit system have 4 distinguishable states corresponding to 4 properly spaced energy levels.

Distinguishability here refers to the possibility of making a distinction between each of the 4 states by measurement. For a fully functioning 2-qubit quantum computer, it is necessary that the 4 qubit states that are functionally orthogonal be experimentally distinguishable. In the current design, the coupled qubits are actualized as two PC qubits weakly coupled by their mutual inductance. In the single qubit case, the DC measurement SQUID measures the state of the qubit through the flux induced by the qubit circulating current in the DC SQUID. The basic idea is unchanged for the coupled qubit system. In this case, there is one DC SQUID that measures the collective state of the coupled qubits through the total induced flux created by both qubits. For example the  $|00\rangle$  state could correspond to qubits 1 and 2 both having counterclockwise circulating current. In this case, the  $|11\rangle$  state would correspond to both qubits with clockwise circulating current. If the individual qubits were measurable with the DC SQUID, then the  $|00\rangle$  and  $|11\rangle$  states of the coupled qubit system should also be measurable because the total qubit flux induced on the DC SQUID is simply the sum of the individual qubit fluxes. The difficulty in measurement comes in differentiating the  $|01\rangle$  and  $|10\rangle$  states.

A difference in the measured flux from the  $|01\rangle$  and  $|10\rangle$  states can come from a difference in the mutual inductance between the individual qubits and the measurement SQUID and/or a difference in the magnitude of the circulating current for the two qubits. Currently, it is not practical to achieve the separation of flux states from adjusting mutual inductance values. Therefore, the approach has been to create two qubits with differing circulating current magnitudes. The magnitude of the circulating current is determined by the size of the junctions. Our analysis shows that there are 6 acceptable qubit parameter choices given the fabrication constraints for a single qubit. Since there are 2 qubits in the coupled qubit

system, there are a total of 15 possible “distinct” coupled qubit combinations. Not all of these 15 possibilities are practical, because some still require rather large qubit-SQUID coupling for distinguishability between the  $|01\rangle$  and  $|10\rangle$  states. The qubit-qubit and qubit-SQUID mutual inductance are parameters that can be varied through choices in geometry. As in the single qubit case, there are inherent tradeoffs in deciding on the appropriate size of the coupling.

The need for properly spaced energy levels comes from the mode of operation of the qubit. The qubits will be rotated, be it individually or collectively, through RF radiation of the appropriate frequency. In the first round of experiments, the signal will come from an off-chip oscillator. For the full functionality of the couple qubit system, it is required that there be 4 non-degenerate energy levels corresponding to the  $|00\rangle$ ,  $|01\rangle$ ,  $|10\rangle$ , and  $|11\rangle$  states and that the 6 possible state transitions have sufficiently different resonant frequencies. If these conditions are met, then pulses with the appropriate linewidth would be able to do universal quantum computation on the 2-qubit system, including the “CNOT” operation. Following along the previous assumption that the coupled qubit system is accurately described as two individual qubits with weak mutual inductive coupling, it should be clear that the  $|00\rangle$  and  $|11\rangle$  states (corresponding to both qubits in the ground or excited states) should be well separated in energy. To meet the other requirements on the energy levels, the qubit-qubit mutual inductive energy needs to be sufficiently large and the qubits need to have different junction sizes. The latter requirement is already necessitated by the measurement limitations. The former represents another tradeoff in the design, as there are problems if the coupling is too strong. Beyond the aforementioned desiderata, it is necessary that the magnitude of these resonant frequencies be practical for experiments.

For the current fabrication run, there are 6 coupled qubit designs. An effort was made to span the acceptable parameter space for the tradeoffs mentioned above.

## **8. Measurement of Qubit States with SQUID Inductance**

### **Sponsors**

AFOSR grant F49620-01-1-0457 under the DoD University Research Initiative on Nanotechnology (DURINT) program, and by ARDA, and by the National Science Foundation Fellowship

### **Project Staff**

Janice C. Lee, Professor Terry P. Orlando

For the persistent current qubits, the two logical states correspond to currents circulating in opposite directions. The circulating current generates a magnetic flux that can be sensed by a SQUID magnetometer inductively coupled to the qubit. Depending on the state of the qubit, which determines the direction of the persistent current, this additional flux either adds to or subtracts from the background magnetic flux. Therefore, during the readout process, the two qubit states can be distinguished by a difference in magnetic flux signal, typically on the order of a thousandth of a flux quantum.

It is of great consequence that the measurement setup has minimum back-actions on the qubit. The present measurement scheme is the so-called switching current method and has some major drawbacks. It uses the property that the critical current of a SQUID is a function of the magnetic flux that it senses, and hence will be different depending on what state the qubit is in. During the measurement, the value of the critical current is obtained directly by ramping a DC current through the SQUID and determining the point at which it switches from the superconducting state to the finite voltage state. This method requires a high current bias and introduces severe back-actions on the qubit.

The SQUID inductance measurement scheme was proposed to be an improvement over the switching current method [1]. With this method, the current through the SQUID can now be biased significantly below the critical current level, and hence reduces the back-actions on the qubit. The idea is to use the SQUID as a flux-sensitive inductor. Basically, the Josephson inductance across the junctions of the SQUID is also a function of the magnetic flux. To measure the inductance effectively, the SQUID is

inserted in a high Q resonant circuit (fig.1). Note that the circuit is fed by a DC current bias as well as an AC source of a single frequency  $\omega_b$ .

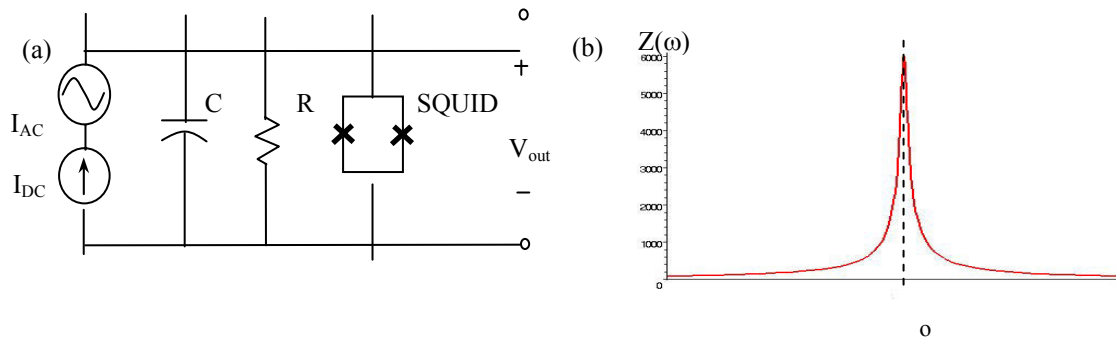


**Figure 1 (a)** A resonant circuit used to measure the SQUID inductance. The ‘x’ represents a Josephson junction. This circuit is simplified from the actual design for illustrative purpose. (b) The corresponding plot of the magnitude of the impedance vs. frequency. The resonant frequency is denoted as  $\omega_0$ .

Upon a change in the qubit state, the corresponding change in the SQUID inductance will shift the resonant frequency (fig.2). This is because the resonant frequency is given by  $1/\sqrt{LC}$ , where  $L$  is the inductance of the SQUID. If one keeps the AC current source at a bias frequency  $\omega_b$ , typically around 500MHz, one senses a change in the impedance  $\Delta Z$ . This in turn results in a difference in the output voltage  $\Delta V$  corresponding to  $I_{AC} \times \Delta Z$ . This voltage difference will be measured to detect the state of the qubit.

High Q resonant circuits were designed with impedance transformation and impedance matching techniques to optimize the measurement process. Detailed calculations were performed for the specific circuits currently being fabricated at the MIT Lincoln Laboratory, and the voltage corresponding to the qubit signal is expected to be about  $10\mu V$ .

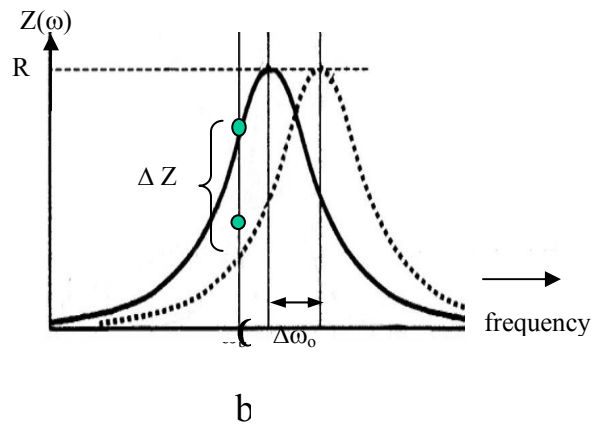


**Figure 2:** Illustration of the shift in resonant frequency  $\Delta\omega_0$  upon a change in the qubit state. During the measurement, one biases the operating frequency at  $\omega_b$  and senses a change in impedance  $\Delta Z$ , which in turn can be retrieved as a voltage signal.

## References:

- [1] Kees Harmans, "Measuring/interrogating a qubit magnetic state employing a dc- SQUID as a flux-sensitive inductor", August 2000.  
[2] Janice C. Lee, "Magnetic flux measurement of superconducting qubits with Josephson inductors", S.M. Thesis, MIT, 2002.

## 9. Type II Quantum Computing Using Superconducting Qubits

### Sponsor

AFOSR grant F49620-1-1-0457 funded under the Department of Defense, Defense University Research Initiative on Nanotechnology (DURINT)

### Project Staff

Professor Terry Orlando, David Berns, Dr. Karl Berggren (Lincoln Laboratory), Jay Sage (Lincoln Laboratory), Jeff Yepez (Air Force Laboratories)

Most algorithms designed for quantum computers will not best their classical counterparts until they are implemented with thousands of qubits. By all measures this technology is far in the future. On the other hand, the factorized quantum lattice-gas algorithm (FQLGA) can be implemented on a type II quantum computer, where its speedups are realizable with qubits numbering only in the teens.

The FQLGA uses a type II architecture, where an array of nodes, each node with only a small number of coherently coupled qubits, is connected classically (incoherently). It is the small number of coupled qubits that will allow this algorithm to be of the first useful quantum algorithms ever implemented.

The algorithm is the quantum mechanical version of the classical lattice-gas algorithm, which can simulate many fluid dynamic equations and conditions with unconditional stability. This algorithm was developed in the 1980's and has been a popular fluid dynamic simulation model ever since. It is a bottom-up model where the microdynamics are governed by only three sets of rules, unrelated to the specific microscopic interactions of the system. The quantum algorithm has all the properties of the classical algorithm but with an exponential speedup in running time.

We have been looking into the feasibility of implementing this algorithm with our superconducting qubits, with long-term plans of constructing a simple type II quantum computer. We currently have a chip scheme to simulate the one dimensional diffusion equation, the simplest fluid dynamics to simulate with this algorithm. The requirements are only two coupled qubits per node, state preparation of each qubit, only one  $\pi/2$  pulse, and subsequent measurement. This can be accomplished with two PC qubits inductively coupled, each with a flux bias line next to it(initialization), and each with a squid around it(measurement), with a tunable (frequency and amplitude) oscillator on-chip next to the two qubits(transformation). All classical streaming will at first be done off-chip.

## 10. Vortex Ratchets

### Personnel

K. Segall, J.J. Mazo, T.P. Orlando

### Sponsors

National Science Foundation Grant DMR 9988832, Fulbright/MEC Fellowship

The concept of a *ratchet* and the *ratchet effect* has received attention in recent years in a wide variety of fields. Simply put a ratchet is formed by a particle in a potential which is asymmetric, i.e. it lacks reflection symmetry. An example is the potential shown in Fig.1, where the force to move a particle trapped in the

potential is larger in the left (minus) direction and smaller in the right (plus) direction. The ratchet effect is when net transport of the particle occurs in the absence of any gradients. The transport is driven by fluctuations. This can happen when the system is driven out of equilibrium, such as by an unbiased AC force or non-gaussian noise. Ratchets are of fundamental importance in biological fields, for study of dissipation and stochastic resonance, in mesoscopic systems, and in our case in superconducting Josephson systems. The key questions are to study how the ratchet potential affects the transport of the particle.

In our group we study the ratchet effect in circular arrays of superconducting Josephson Junctions. In such arrays magnetic vortices or kinks can be trapped inside and feel a force when the array is driven by an external current. The potential that the vortex feels is given by a combination of the junction sizes and the cell areas; by varying these in an asymmetric fashion we can construct a ratchet potential for a vortex. The picture in Fig. 1 is of one of our fabricated circular arrays; the potential shown in Fig. 1 is the numerically calculated potential for a kink inside the array. We have verified the ratchet nature of the potential with DC transport measurements, published in early 2000.

This work is now moving in the quantum direction: smaller junction arrays where quantum effects are important. A quantum ratchet will display new behavior as the temperature is lowered, as both the ratchet potential and quantum tunneling can contribute to the kink transport. We have designed and fabricated such arrays and are presently testing them. The experiments we do in these newer devices is to measure the switching current, which is the current that is required to cause the vortex to depin and the system to switch to a running mode or finite voltage state. In the mechanical analog it represents the critical force to move the particle, and in a ratchet potential it is different in one direction than the other. For a classical ratchet, the direction with the lower critical force will always have the larger depinning rate. However, in a quantum ratchet the direction with the lower transition rate will depend on the temperature. A crossover in the preferred direction, the direction with the larger depinning rate, is the signature of possible quantum behavior. In Fig. 2 we show the switching current as a function of temperature for the two directions. A crossover is clearly seen. We are in the process of doing further experiments and calculations to verify that we have truly made a quantum ratchet.

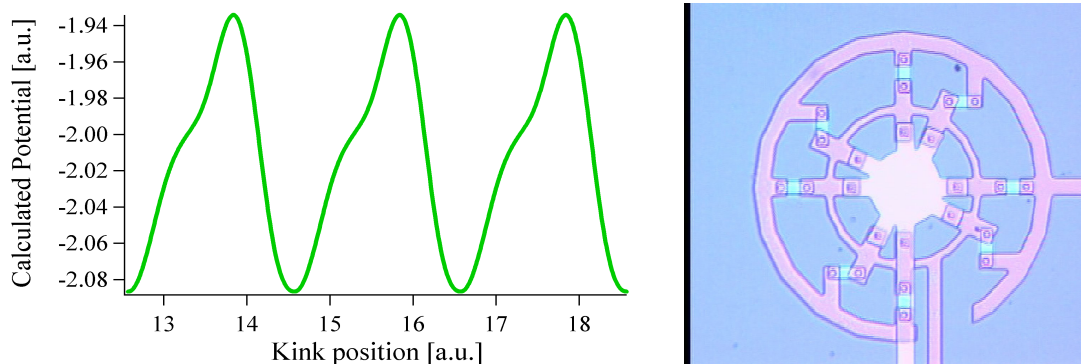


**Fig. 1:** A ratchet potential and its realization in a Josephson array. The array has alternating junction sizes and plaquette areas to form the asymmetric potential for a vortex trapped inside the ring. The outer ring applies the current such that the vortex transport can be measured. The potential is numerically calculated for the array parameters.

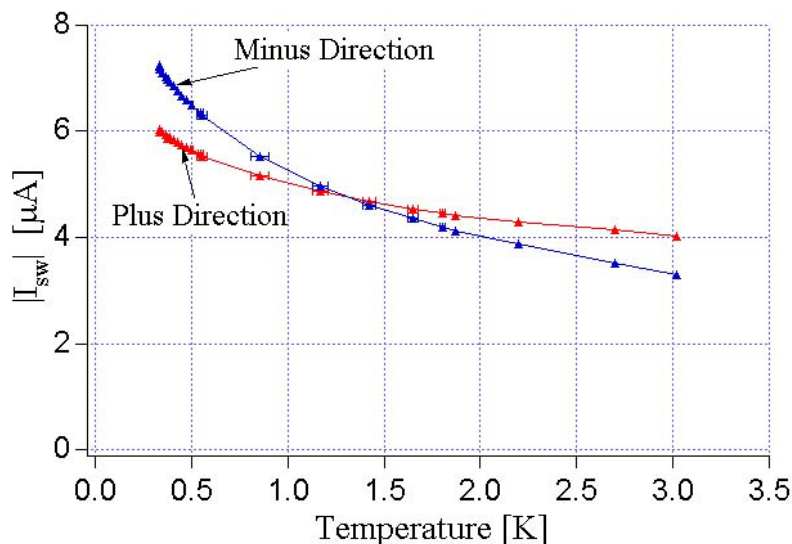


**Fig. 2:** Switching current for the plus and minus direction of a circular, 1-D Josephson array fabricated in the quantum regime. The switching current is a measure of the depinning rate in each direction. The crossover indicates that the preferred direction changes as a function of temperature. This is a possible signature of quantum effects.

## 11. Interaction between discrete breathers and other non-linear modes in Josephson arrays

### Sponsorship

National Science Foundation Grant DMR 9988832  
 Fulbright/MEC Fellowship

### Personnel

Dr. Kenneth Segall, Dr. J.J. Mazo, Professor Terry P. Orlando

Linear models of crystals have played a fundamental role in developing a physical understanding of the solid state. However, many phenomena are unexplained until one considers non-linear interactions. One particularly interesting phenomenon is that of *discrete breathers*, which are time periodic, spatially localized modes. In a crystal a discrete breather is localized in that a few atoms are vibrating while the neighboring atoms stay still. Josephson junctions are a solid state realization of non-linear oscillators and they can experimentally be coupled in various ways using standard lithographic fabrication techniques. In figures 1A and 1B we show a regular array of Josephson junctions, denoted by x's, which are driven by a uniform current (driving current not shown). Each junction is governed by equations isomorphic to a damped pendulum; the phase of the pendulum is equivalent to the superconducting phase difference across the junction. A discrete breather is shown in 1B, where a few of the junctions have their phases rotating in time while the others do not. Experimentally a rotating phase corresponds to a net DC voltage, which can be easily measured. Breathers in Josephson arrays have been studied in previous work in our group here at MIT.

In Fig. 1A we demonstrate another kind of non-linear mode, a *moving vortex*. This is mathematically equivalent to a kink or solitonic mode. Vortices in Josephson arrays carry a quantum of magnetic flux and have been studied extensively in superconducting systems. A vortex corresponds to a  $2\pi$  phase shift in the phases of the vertical junctions in the ladder; when a uniform current is applied the vortex moves down the ladder. As the vortex passes a given junction it causes its phase to undergo a rotation and thus create a voltage. This is indicated by the time sequence shown in Fig. 1A.

Our work is aimed at studying the interaction of discrete breathers with other kinds of non-linear modes, like a moving vortex. Such questions are of fundamental importance for the Non-linear Dynamics community. In Fig. 2 we show a mathematical simulation of a collision between a vortex and a breather. The vertical axis is the junction number in the array; the array in the simulation has 60 junctions. The horizontal axis is time. The color indicates the junction voltage or rotation speed, with blue indicating low voltage and red indicating high voltage. Initially there is a breather located about junction 10 and a vortex located in junction 45. As time proceeds the vortex moves toward the breather and eventually collides with it. The result of the collision is that the breather acts as a pinning center for the vortex. As time proceeds further (not shown) the vortex will eventually depin and cause the breather to decay into a different mode. We have also seen other collision scenarios in our simulations, such as ones where the breather is destroyed or where the breather pins a train of moving vortices. We are also looking for such behavior experimentally, with fabricated junction arrays and DC electronics.

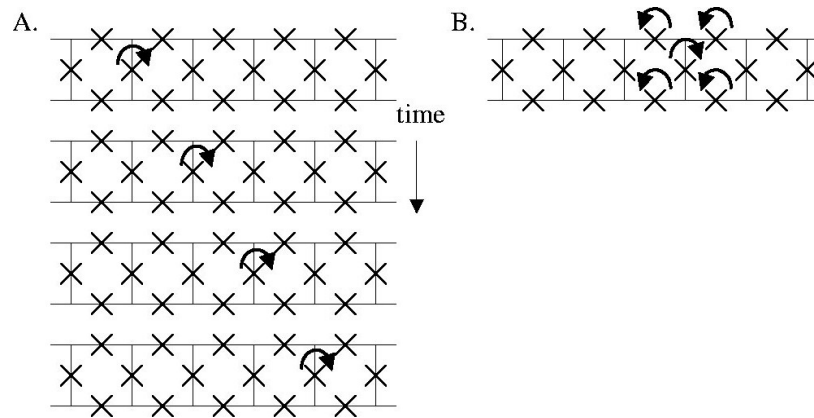


**Fig. 1:** Representation of two different non-linear modes in a Josephson Ladder: (a) Moving vortex: The vortex causes the phase of a junction to rotate as it passes by. (b) Discrete breather: A few junctions have their phases continually rotating while the neighboring ones do not.

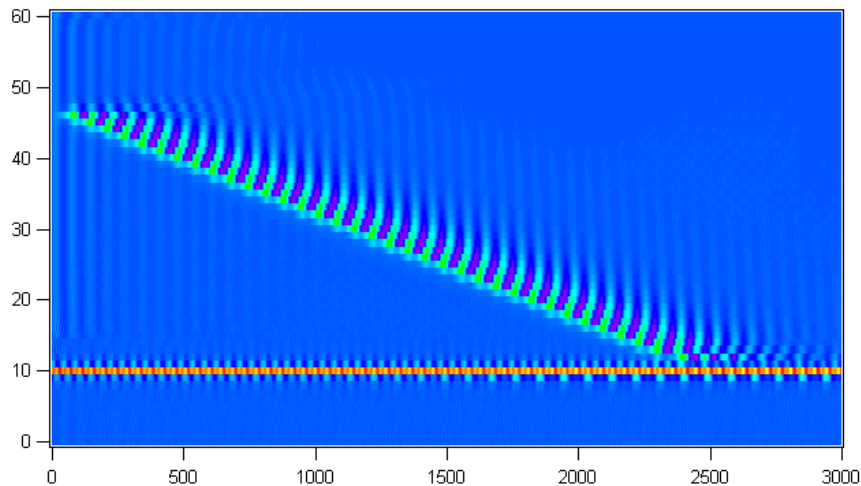


**Fig. 2:** Interaction of a breather with a moving vortex. Time (in arbitrary units) is on the horizontal axis, the junction number is on the vertical axis, and the color indicates the junction voltage (red=high, blue=low). The vortex starts in junction 45 and moves toward the breather, which is in junction 10. The vortex collides with the breather and is pinned by it, with the breather surviving at later times.

### **Journal Articles, Published**

William M. Kaminsky and Seth Lloyd, “Scalable Architecture for Adiabatic Quantum Computing of NP-hard problems, in Quantum computing and Quantum Bits in Mesoscopic Systems, Kluwer Academic 2003.

Lin Tian, Seth Lloyd, and T. P. Orlando, “Projective Measurement Scheme for Solid-State Qubits,” submitted to Physical Review B 2003.

K. Segall, D. Crankshaw, D. Nakada, T. P. Orlando, L. S. Levitov, S. Lloyd, N. Morkovic, S. O. Valenzuela, M. Tinkham, and K. K. Berggren. “Impact of time-ordered measurements of the two states in a niobium superconducting qubit structure,” submitted to Physical Review B.

K. Segall, D. S. Crankshaw, D. Nakada, B. Singh, J. Lee, T. P. Orlando, K. K. Berggren, N. Markovic, M. Tinkham, "[Experimental characterization of the two current states in a Nb persistent-current qubit](#)," accepted for publication in *IEEE Trans. Appl. Supercon.* (2003).

K. Berggren, D. Nakada, T.P. Orlando, E. Macedo, R. Slattery, and T. Weir, “An integrated superconductive device technology for qubit control,” submitted for publication.

L. Tian, S. Lloyd and T.P. Orlando, “Decoherence and Relaxation of Superconducting Persistent-Current Qubit During Measurement “, accepted by *Phys. Rev. B.* (2002);

Lin Tian, “A Superconducting Flux QuBit: Measurement, Noise and Control,” PhD Thesis, 2002;

Janice Lee, “Magnetic Flux Measurement of Superconducting Qubits with Josephson Inductors,” MS Thesis, 2002.